THE INFLUENCE OF GLOBAL SEA SURFACE TEMPERATURE ON THE 1988 U.S. DROUGHT: A Comparison of Simulations With Two General Circulation Models

M. J. Fennessy, L. Marx, J. L. Kinter III and J. Shukla

Center for Ocean–Land–Atmosphere Interactions
Department of Meteorology
University of Maryland
College Park, Maryland 20742, USA

1. INTRODUCTION

During the spring and early summer of 1988, widespread severe drought conditions existed over much of the eastern and central U. S. Concurrently, significant anomalies were observed in the global sea surface temperature (SST) field in several regions. In the central and eastern tropical Pacific warm (El Niño) SST anomalies lasted until March, after which cold (La Niña) SST anomalies persisted throughout the remainder of the year.

Trenberth et al. (1988) analyzed the atmospheric circulation patterns observed during May and June 1988 and identified patterns in the anomalous 500 mb geopotential height field resembling dispersion of Rossby waves emanating from the central and eastern tropical Pacific towards the northeast Pacific and North America. A strong ridge over the central U. S. related to the downstream surface drought conditions was one part of this pattern. Trenberth et al. (1988) forced a simple atmospheric model with idealized heating anomalies derived from the anomalous outgoing longwave radiation (OLR) observed during May and June 1988, and obtained a wave train over the Pacific and North America resembling that observed. Given the well known link between tropical SST and convective heating, Trenberth et al. (1988) hypothesized that the SST anomalies in the tropical Pacific forced an anomalous Rossby wave train which resulted in upper level ridging over the central U. S. and drought conditions below.

In the current study, we investigate possible relationships between the global SST and the atmospheric circulation patterns observed during May and June 1988, using two different atmospheric general circulation models (GCMs). This differs from the Trenberth et al. (1988) study in that we are forcing full atmospheric GCMs with only the observed SST, and in that we are using the entire global SST field, rather than only the tropical Pacific SST directly related to the idealized heating anomalies used by Trenberth et al. (1988).

2. EXPERIMENT AND MODELS

To investigate a possible link between global SST and the 1988 U.S. drought, integrations were performed with two very different atmospheric GCMs. This approach was expected to yield some indication of the model dependency of the results and give insight into the importance of correctly simulating various features of the observed time mean atmospheric circulation. The Goddard Laboratory for Atmospheric Sciences (GLAS) GCM was used because of its past success in simulating the atmospheric response to El Niño tropical Pacific SST anomalies (Fennessy et al., 1985; Shukla and Fennessy, 1988). The GLAS GCM is a global grid point model with a 4 degree latitude by 5 degree longitude grid and 9 sigma levels in the vertical. The PBL is that of Deardorff (1972) as modified by Randall (1976). Supersaturation clouds occur at all 9 levels, while convective clouds (Arakawa, 1969) are limited to the lowest 6 levels. Only the bottom 6 levels of supersaturation clouds interact with radiation.

The Center for Ocean–Land–Atmosphere Interactions (COLA) R40 GCM was used because of its overall superior performance, particularly for summer simulations. The superiority of the COLA GCM summer simulations will be demonstrated by comparisons with observations and with the GLAS GCM simulations in the results section. The extent of this superiority was not fully realized by the authors before this study was begun. The COLA GCM was derived from a version of the National Meteorological Center (NMC) Medium Range Forecast (MRF) spectral GCM, retaining the NMC spectral dynamics with rhomboidal truncation at total wave number 40 (Sela, 1980). The GCM has undergone several revisions and is different from the version described by Kinter et al. (1988). It has 18 unevenly spaced sigma levels in the vertical with tighter spacing near the PBL and tropopause. The PBL parameterization is a modified version of Deardorff (1972). The convection scheme is that of Kuo (1965) and shallow convection (Tiedtke et al., 1984) is also included. The longwave radiation scheme is based on that of Harshvardhan and Corsetti (1984) and the shortwave radiation scheme follows that of Lacis and Hansen (1974). This version of the GCM carries moisture at only the lowest 12 sigma levels and only prescribed zonally symmetric clouds interact with the radiation schemes.

Each GCM was integrated for three 60–day pairs, initialized from the observed atmospheric states on 1, 2, and 3 May 1988, respectively. Each pair consists of a control integration with global time–varying climatological SST specified and a boundary integration with global time varying observed SST for 1988. Non–interactive time–varying climatological soil moisture and surface albedo were used in all integrations.

3. RESULTS

The anomalous May 1988 SST field (Fig. 1a) contains over 2° C cold La Niña SST anomalies in the central and eastern Pacific, flanked by 0.5 to 1° C warm anomalies to the north and south. There are also 0.5 to 1° C warm anomalies in the equatorial western Pacific, Atlantic and Indian oceans, which may be important due to the very warm (28° C) May climatological SST in these areas (Fig. 1b), and the well known relation between very warm tropical SST and intense convection (Graham and Barnett, 1987).

The May–June mean (MJ) ensemble mean of the 3 boundary (observed SST) simulations of each GCM is compared to the MJ observations in order to consider the veracity of each GCM in simulating relevant atmospheric circulation features. The MJ boundary minus control ensemble differences of each GCM are compared to the observed MJ

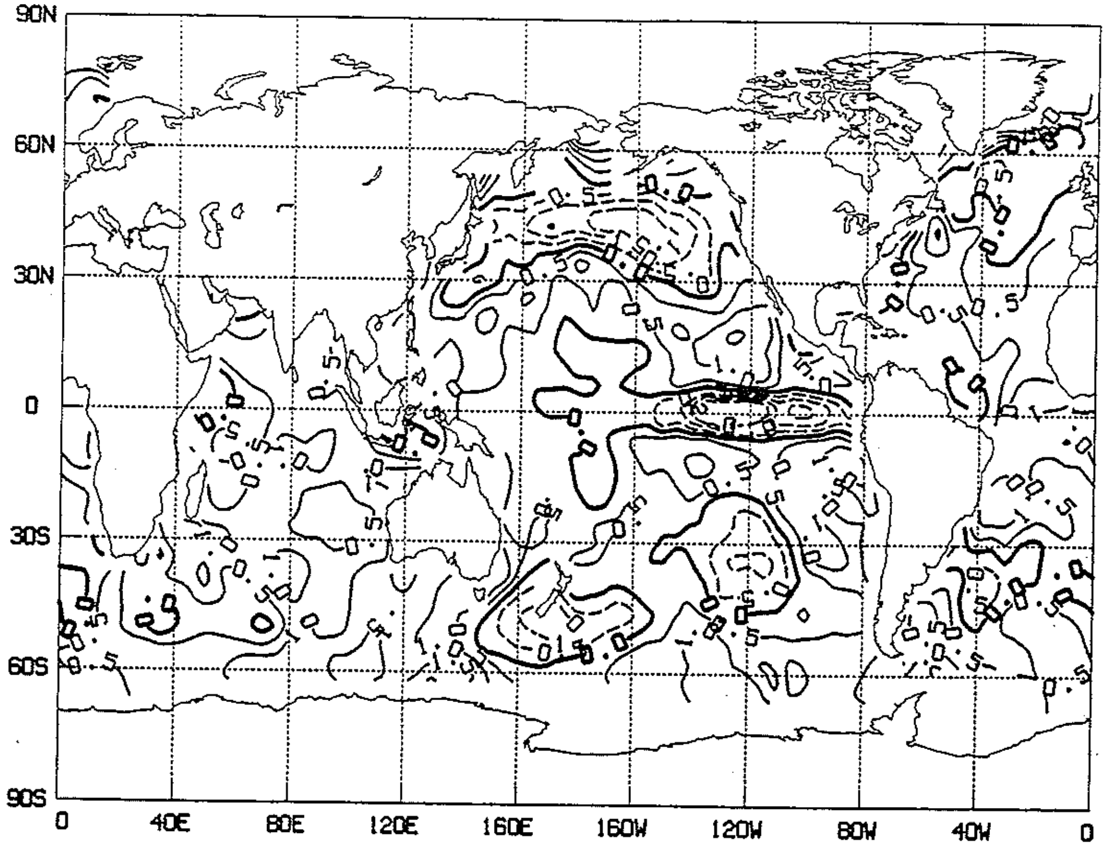

Figure 1a: Observed May 1988 sea surface temperature anomaly. Contour interval is 0.5° C. Dashed contours are negative.

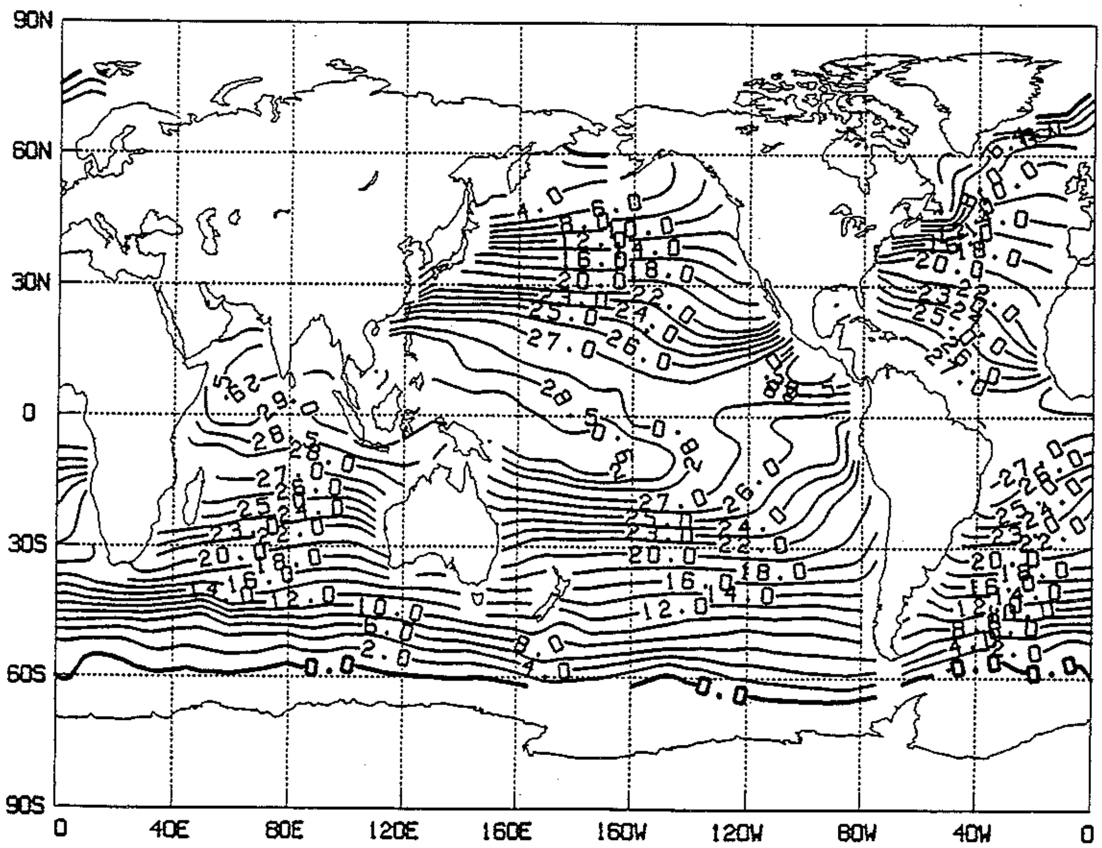

Figure 1b: Observed May 1988 sea surface temperature mean. Contours are 4, 6, 8, 10, 12, 14, 16, 18, 20, 22, 24, 26, 27, 28, 28.5, 29, 30° C. Dashed contours are negative.

atmospheric anomalies. Thus, these simulated anomalies reflect only the effect of using real SST as opposed to using climatological SST. Sixty–day means are used to better demonstrate the effect of the anomalous SST (Baumhefner et al., 1988; Fennessy and Shukla, 1991). All observations shown are time means of NMC analyses, with the exception of the precipitation. The observed anomalies are formed by subtracting the mean of MJ NMC analyses for the ten years 1979 through 1988 from the MJ mean NMC analyses for 1988.

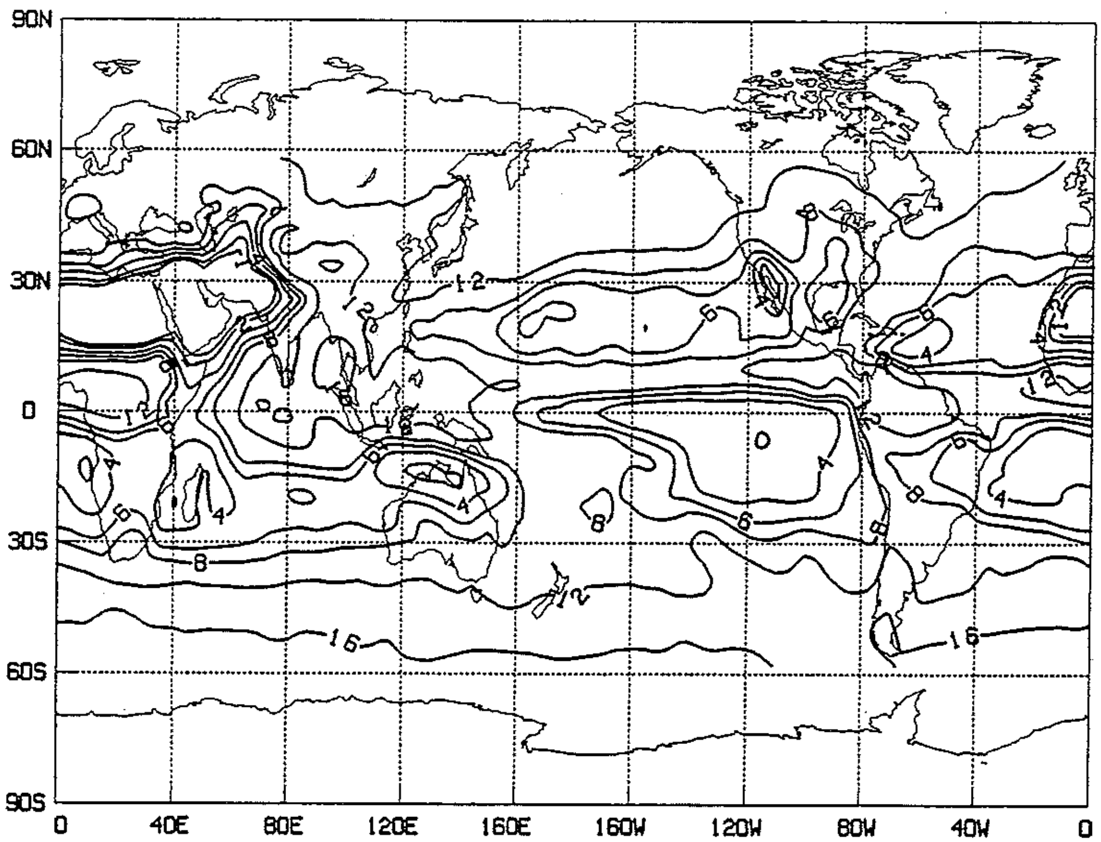

Figure 2a: MJ 1988 precipitation for observed mean calculated from OLR. Contours are 1, 2, 4, 6, 8, 12, 16, 20, 24, 28 mm day^{-1}.

The observed MJ 1988 mean precipitation (Fig. 2a) is obtained from the OLR via an empirical approximation (Arkin, personal communication). This precipitation proxy becomes less reliable with distance from the equator and should probably only be considered over ocean points within 30 degrees of the equator. The GLAS GCM successfully simulates the Pacific ITCZ and the precipitation maxima over Africa,

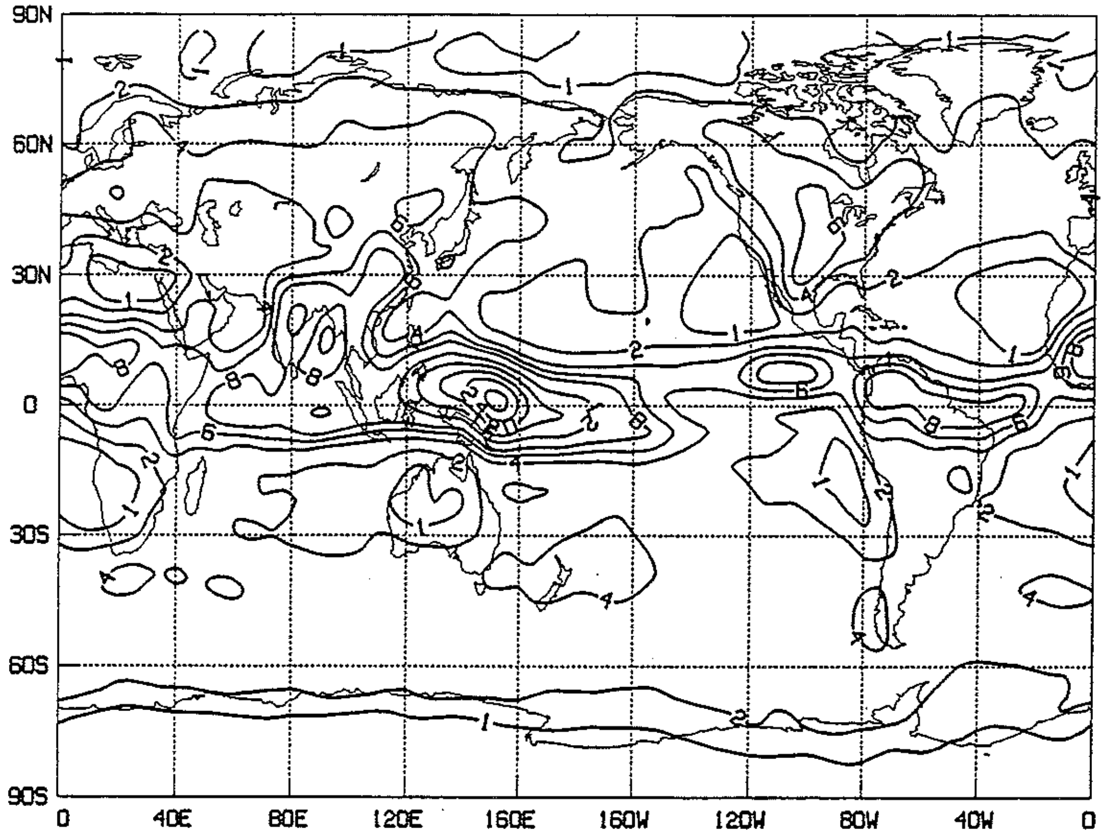

Figure 2b: MJ 1988 precipitation for GLAS boundary ensemble mean. Contours are 1, 2, 4, 6, 8, 12, 16, 20, 24, 28 mm day^{-1}.

India–East Asia and northern South America (Fig. 2b). However, the Pacific ITCZ is somewhat weak, there is no South Pacific Convergence Zone (SPCZ), and far too much precipitation occurs in the west Pacific and over the U.S. The COLA GCM more accurately simulates the ITCZ, SPCZ and tropical precipitation maxima, although it produces too little precipitation in the far west Pacific and also has excessive precipitation over the U.S. (Fig. 2c).

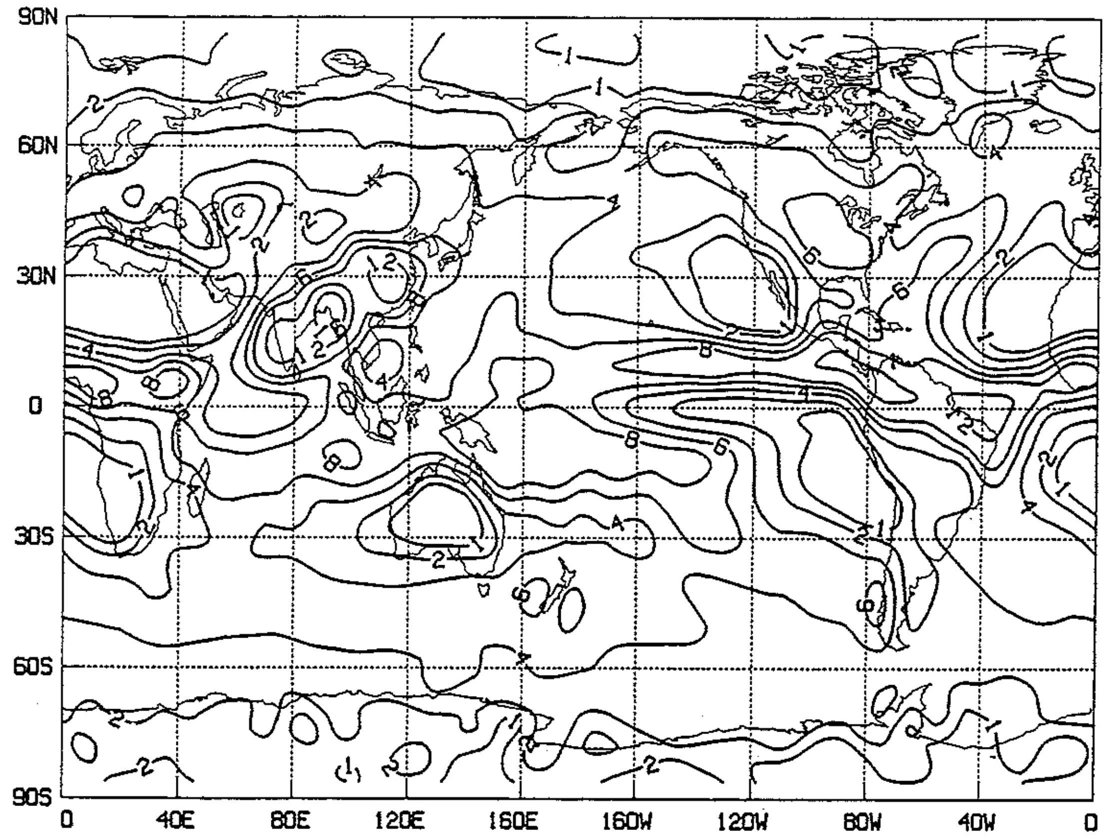

Figure 2c: MJ 1988 precipitation for COLA boundary ensemble mean. Contours are 1, 2, 4, 6, 8, 12, 16, 20, 24, 28 mm day^{-1}.

The observed MJ 1988 precipitation anomaly (Fig. 3a) is obtained from the 1988 OLR and a 15 year OLR climatology via another empirical approximation (Arkin, personal communication). The GLAS GCM correctly simulates most of the observed tropical anomaly features, including the elongated negative anomaly and flanking positive anomalies in the central and eastern Pacific, and the positive anomalies in the western

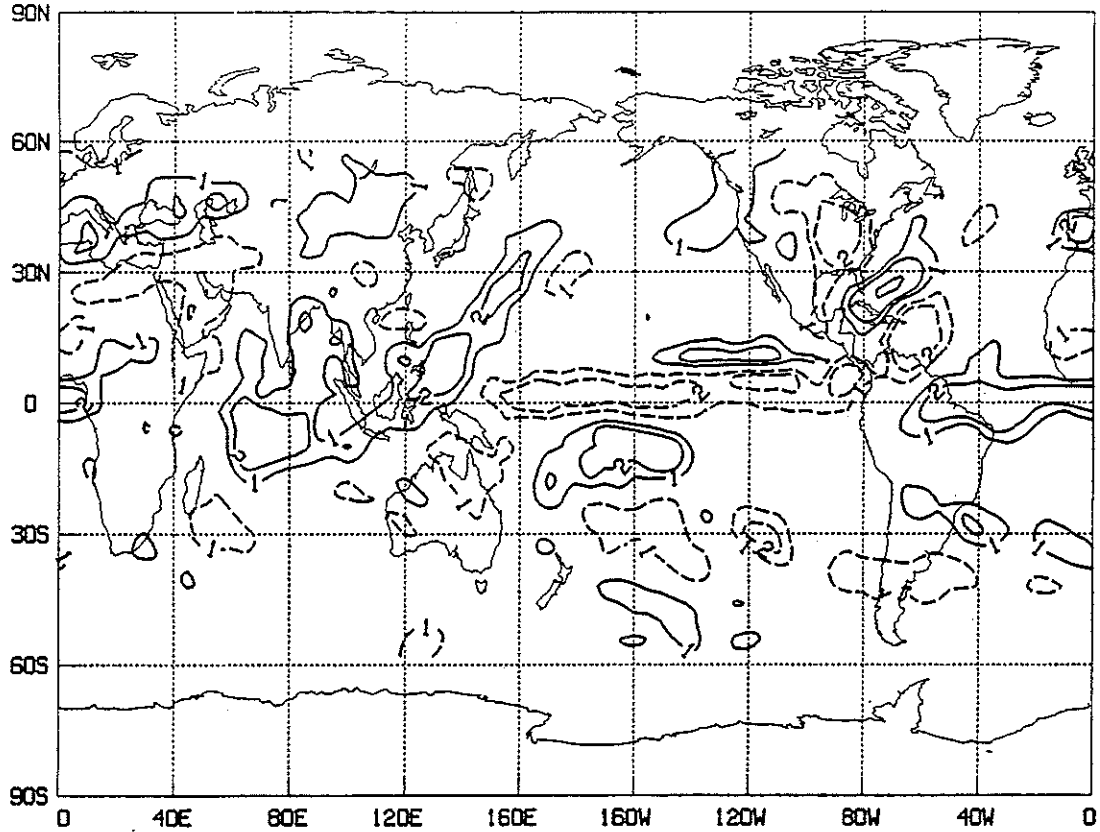

Figure 3a: MJ 1988 precipitation for observed anomaly calculated from OLR anomaly. Contours are ± 1, 2, 4, 8 mm day^{-1}. Dashed contours are negative.

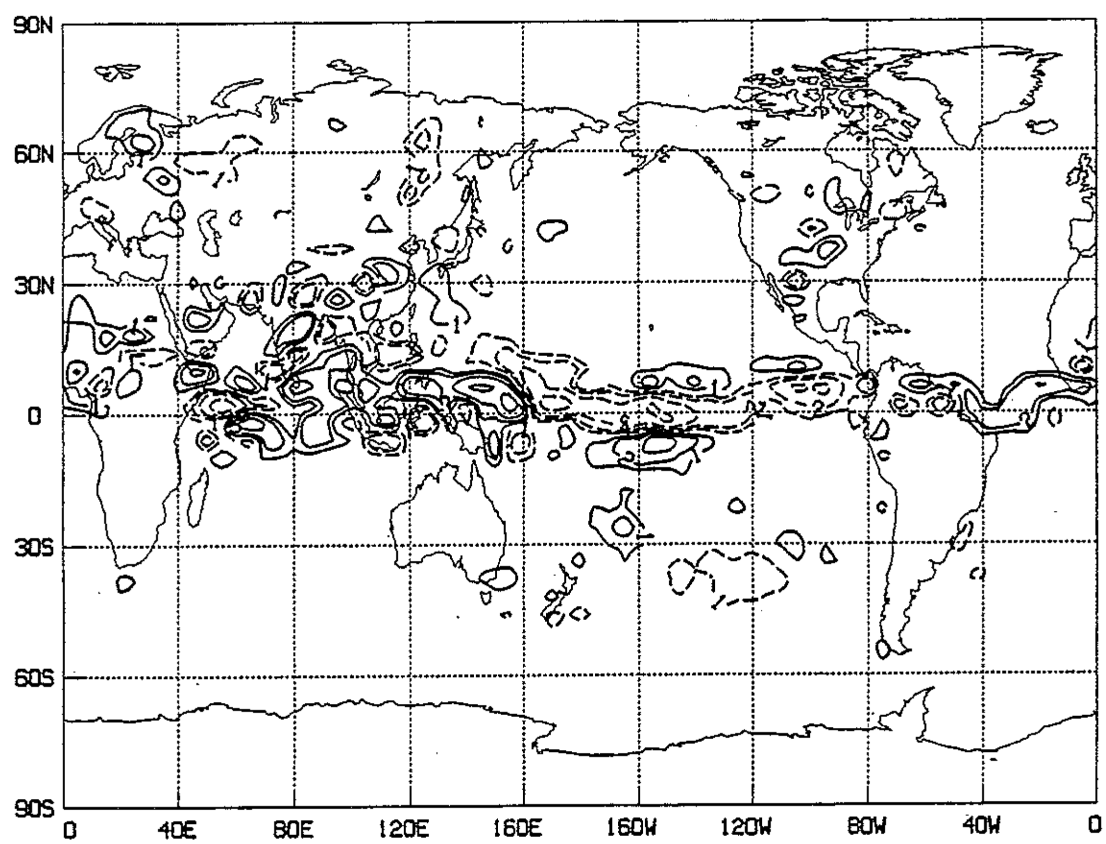

Figure 3b: MJ 1988 precipitation for GLAS simulated anomaly. Contours are ± 1, 2, 4, 8 mm day^{-1}. Dashed contours are negative.

Pacific, Indian, and Atlantic Oceans (Fig. 3b). The COLA GCM also correctly simulates most of these features, and has a better representation of the positive precipitation anomaly in the eastern Pacific at 10–15° N, which Trenberth et al. (1988) suggested was

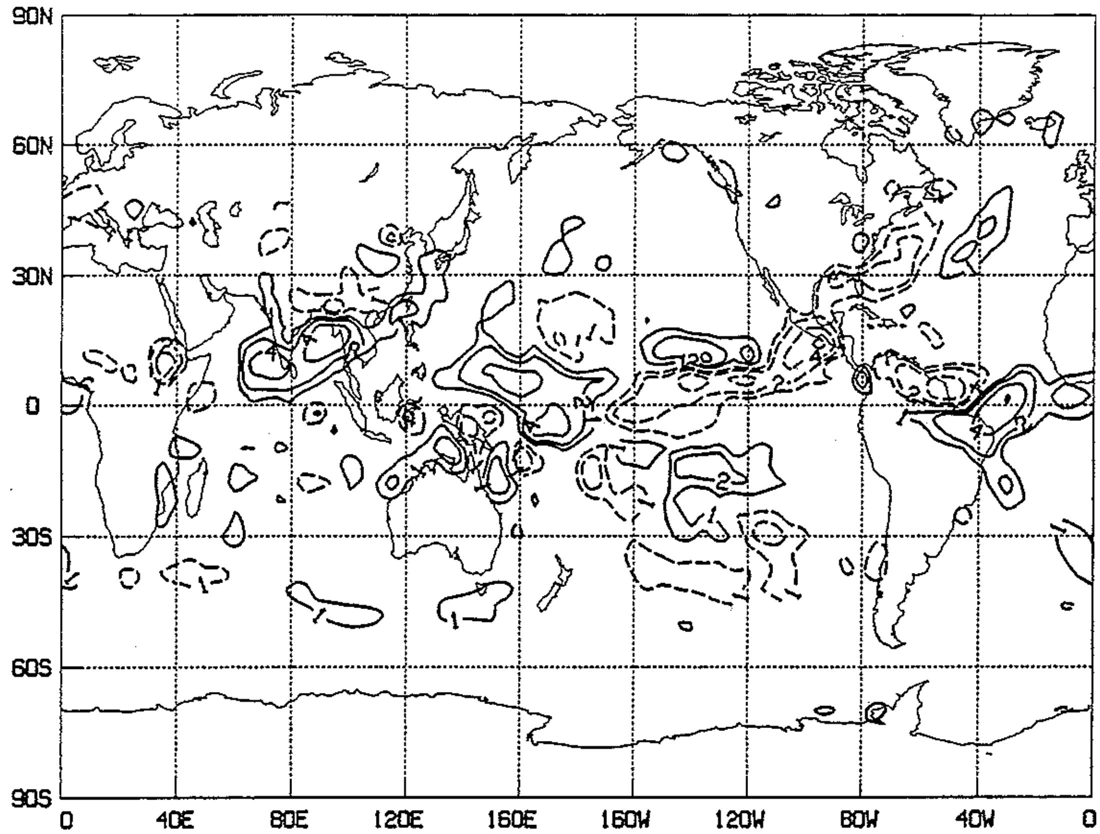

Figure 3c: MJ 1988 precipitation for COLA simulated anomaly. Contours are ± 1, 2, 4, 8 mm day^{-1}. Dashed contours are negative.

dominant in forcing the extra–tropical wave train associated with the U.S. drought. However, the COLA GCM negative anomaly in the equatorial Pacific does not extend as far westward as observed, and its positive anomaly in the western Pacific extends too far eastward (Fig. 3c). Over the U.S., neither one of the GCM precipitation anomaly fields contains the 1988 U.S. drought signal. The COLA GCM does have a large negative signal in the vicinity, but it is eastward of that observed, centered over the Gulf Stream.

In order for the GCMs to correctly force the upper level extra–tropical circulation, their precipitation and heating anomalies must result in divergence anomalies in the upper troposphere. An examination of the anomalous divergence fields for these two GCMs reveals that the COLA GCM maximum divergence anomalies at 200 mb are well correlated with its precipitation anomalies, including those in the central Pacific, while those for the GLAS GCM are weak at the 200 mb level and correspond only to its precipitation anomalies in the western Pacific (not shown). Thus, the COLA GCM does a much better job than the GLAS GCM of converting its precipitation anomalies into divergence anomalies in the upper troposphere where they can effectively force the extra–tropical circulation.

Given an upper troposphere tropical divergence anomaly, Rossby wave dispersion into the extra–tropics is dependant upon the structure of the mean atmospheric flow in the upper troposphere (Branstator, 1983). Of particular importance are the extent of the tropical easterlies (Webster and Holton, 1982) and the structure of the local subtropical jet (Sardeshmukh and Hoskins, 1988). The MJ 1988 300 mb zonal wind is shown for the observations, the GLAS GCM, and the COLA GCM in Figs. 4a, 4b, and 4c, respectively. In the GLAS GCM, the extent of the tropical easterlies is smaller than observed and the northern Pacific subtropical jet is very weak and westward shifted. The COLA GCM does a much better job of simulating both of these features, particularly the subtropical jet, which greatly resembles that observed. The COLA GCM tropical easterlies are, however, more extensive than those observed, and the GCM fails to simulate the westerly duct in the central Pacific. This does not preclude the possibility of Rossby wave dispersion into the Northern Hemisphere in the COLA GCM; as a Rossby wave source in the subtropics may be formed by the advection of absolute vorticity by the divergent wind (Sardeshmukh and Hoskins, 1988).

4a

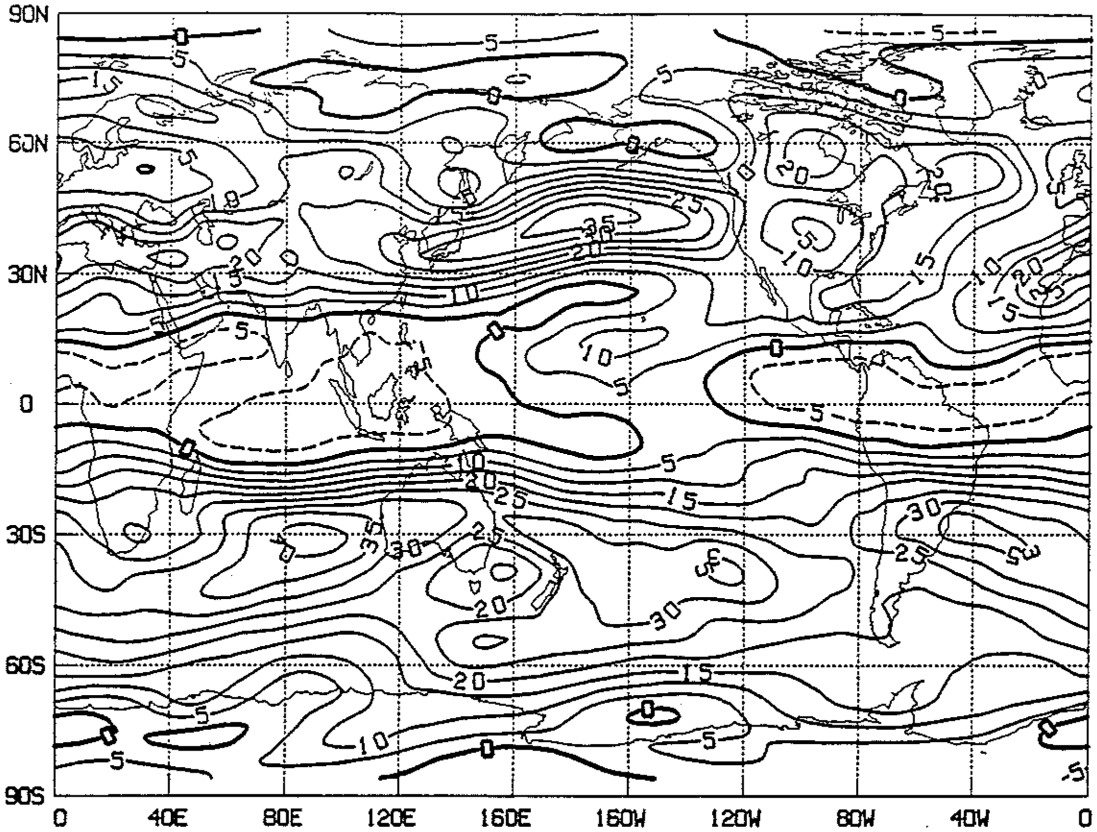

Figure 4a: MJ 1988 zonal wind at 300 mb for NMC observed mean. Contour interval is 5 m s^{-1}. Dashed contours are negative.

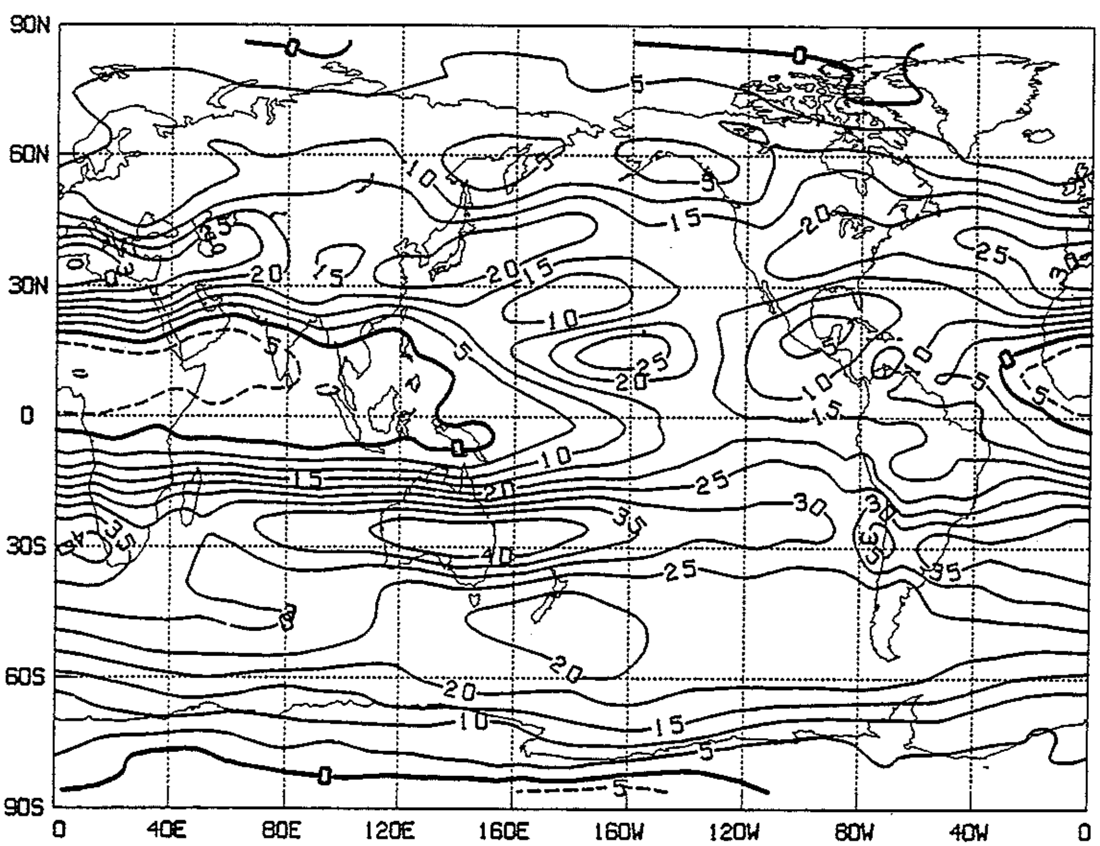

Figure 4b: MJ 1988 zonal wind at 300 mb for GLAS boundary ensemble mean. Contour interval is 5 m s^{-1}. Dashed contours are negative.

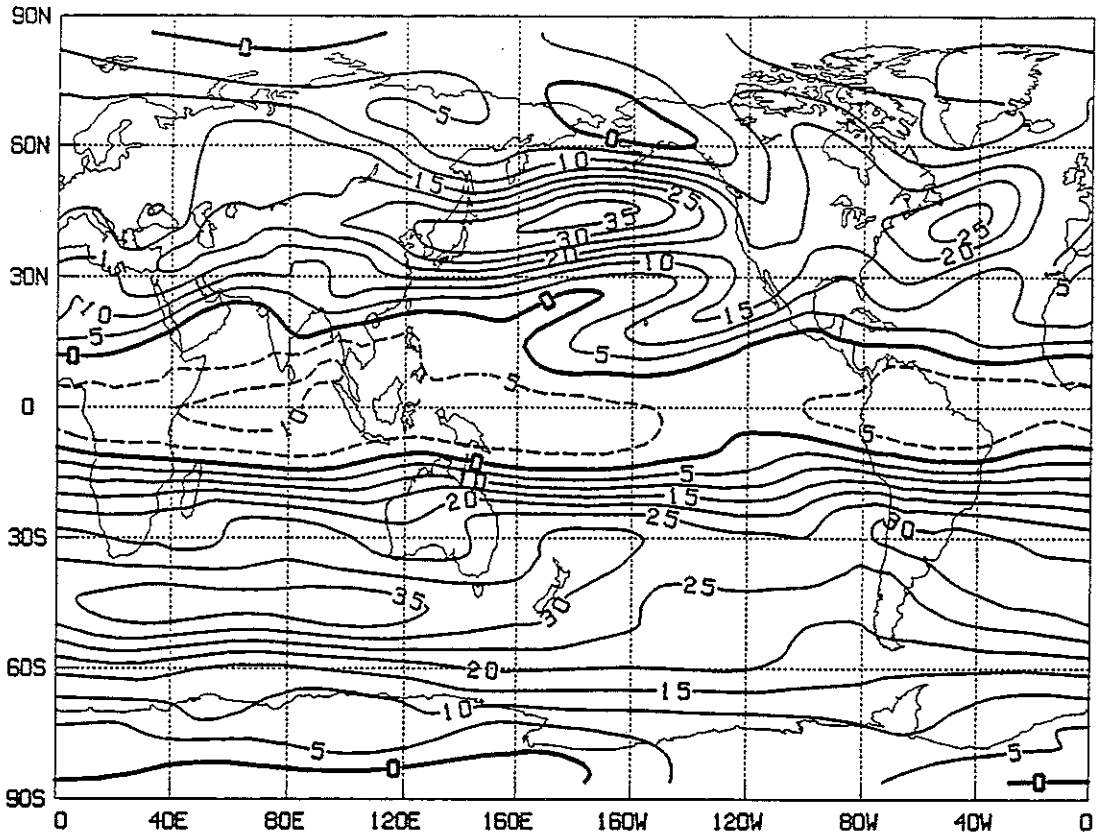

Figure 4c: MJ 1988 zonal wind at 300 mb for COLA boundary ensemble mean. Contour interval is 5 m s^{-1}. Dashed contours are negative.

The advection of absolute vorticity by the divergent wind at 200 mb (hereafter AVD) was calculated for the MJ 1988 control and boundary ensembles of each GCM. We show only the anomaly (boundary ensemble mean minus control ensemble mean) for the GLAS GCM (Fig. 5a) and the COLA GCM (Fig. 5b). It should be noted that this is just one of the two components of the effective Rossby wave source defined by Sardeshmukh and Hoskins (1988). The GLAS GCM AVD anomalies are quite weak, with coherent signals appearing only over the western Pacific (15° N, 140° E–160° W), just north of its strongest 200 mb divergence anomalies. The COLA GCM produces coherent AVD anomalies to the

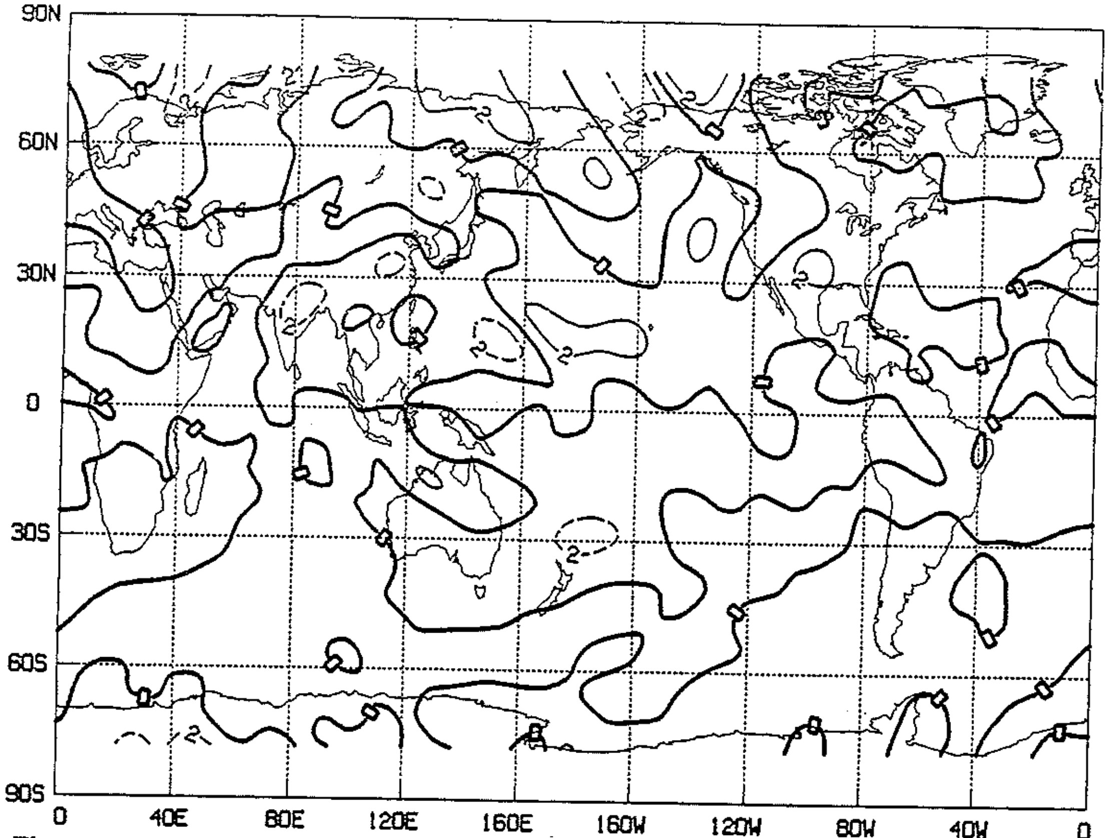

Figure 5a: MJ 1988 advection of absolute vorticity by the divergent component of the wind at 200 mb for GLAS simulated anomaly. Contour interval is 2 x 10^{-11} s^{-2}. Dashed contours are negative.

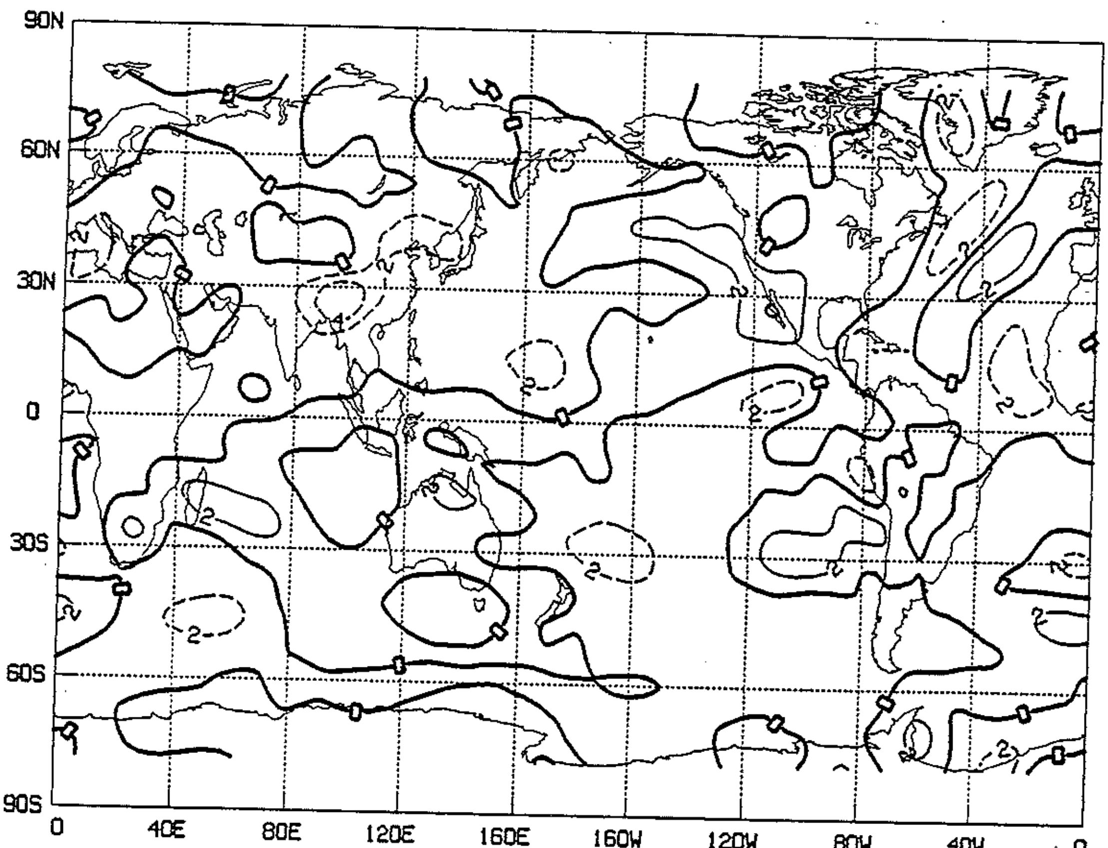

Figure 5b: MJ 1988 advection of absolute vorticity by the divergent component of the wind at 200 mb for COLA simulated anomaly. Contour interval is 2 x 10^{-11} s^{-2}. Dashed contours are negative.

north of its tropical precipitation and 200 mb divergence anomalies in the eastern Pacific, the Atlantic, and the eastern Indian – western Pacific Oceans. This suggests that all 3 regions may be important in forcing the COLA GCM Northern Hemisphere extra–tropics via Rossby wave dispersion during MJ 1988.

The observed MJ 1988 300 mb geopotential height anomaly field (Fig. 6a) contains a wave train pattern emanating from the central and eastern Pacific and arching over North America as noted by Trenberth et al. (1988). Part of this pattern is the large (150 m) positive anomaly over the north–central U.S. and Canada which is associated with the 1988

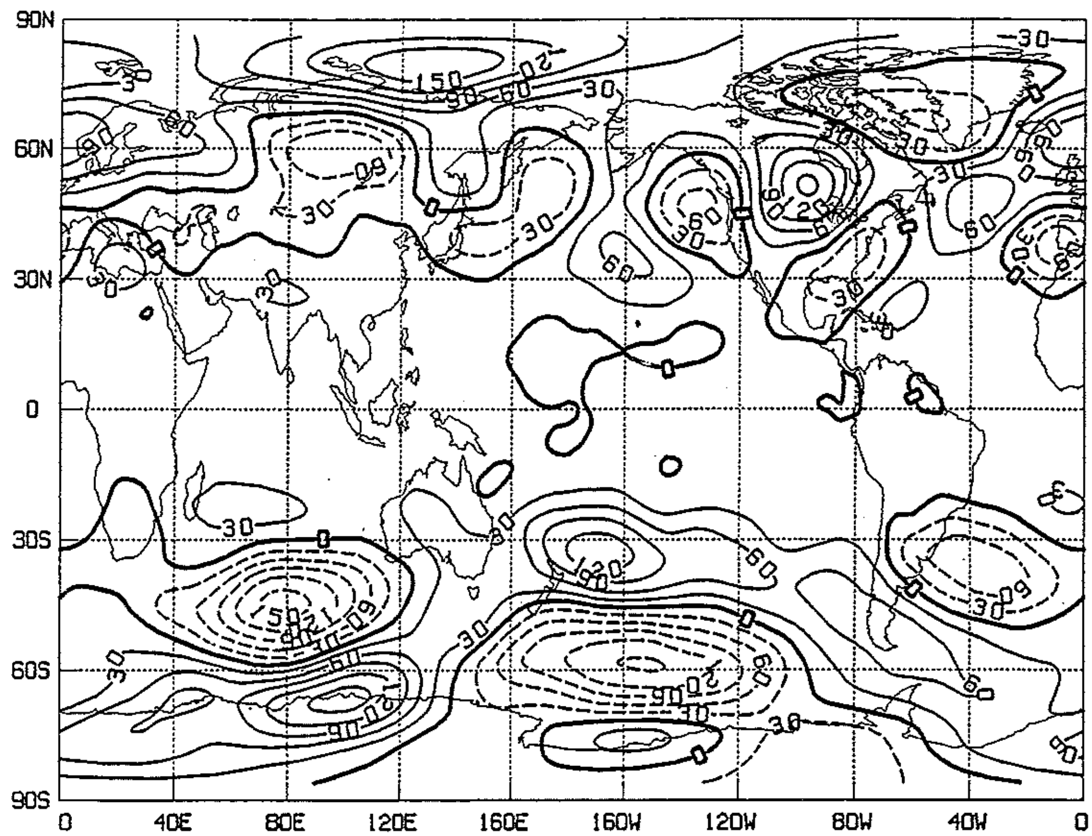

Figure 6a: MJ 1988 geopotential height at 300 mb for NMC observed anomaly. Contour interval is 30 m. Dashed contours are negative.

U.S. drought. The GLAS GCM anomaly field is completely missing this wave train pattern and has only very weak anomalies over the entire region (Fig. 6b). The COLA

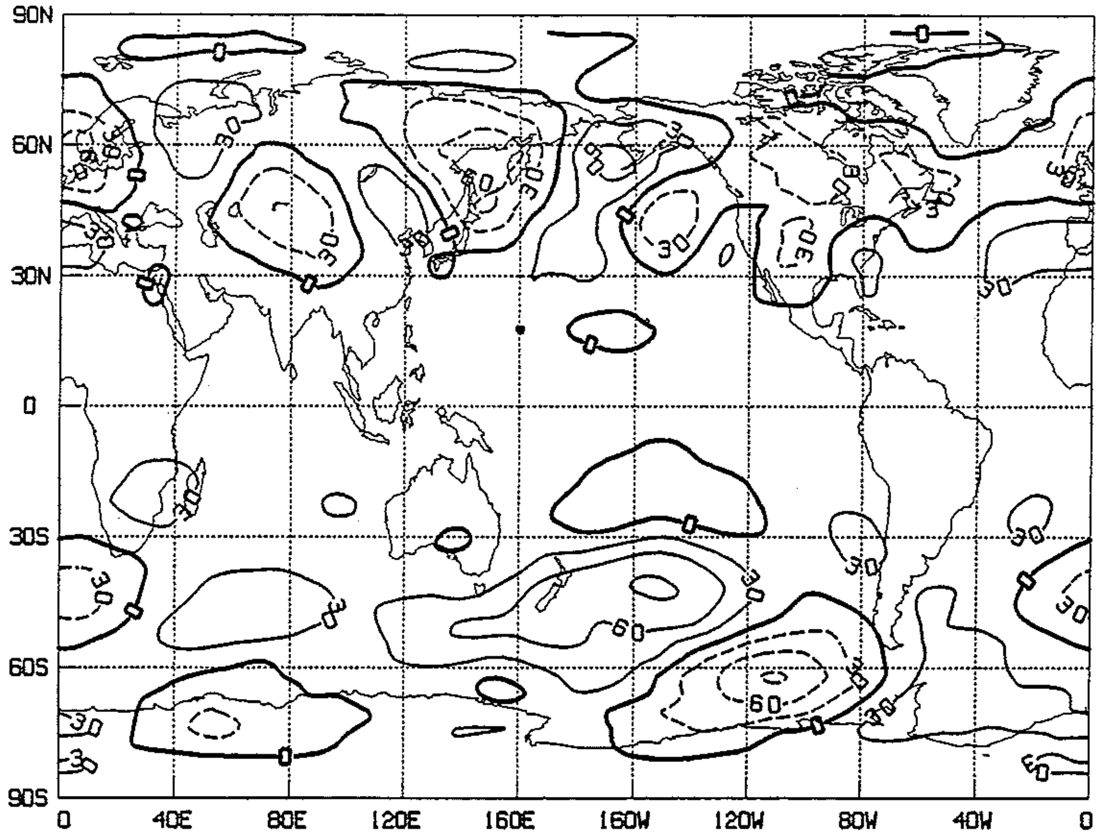

Figure 6b: MJ 1988 geopotential height at 300 mb for GLAS simulated anomaly. Contour interval is 30 m. Dashed contours are negative.

GCM 300 mb geopotential height anomaly field contains a wave train pattern which is somewhat similar to that observed, albeit weaker and eastward (Fig. 6c). The COLA

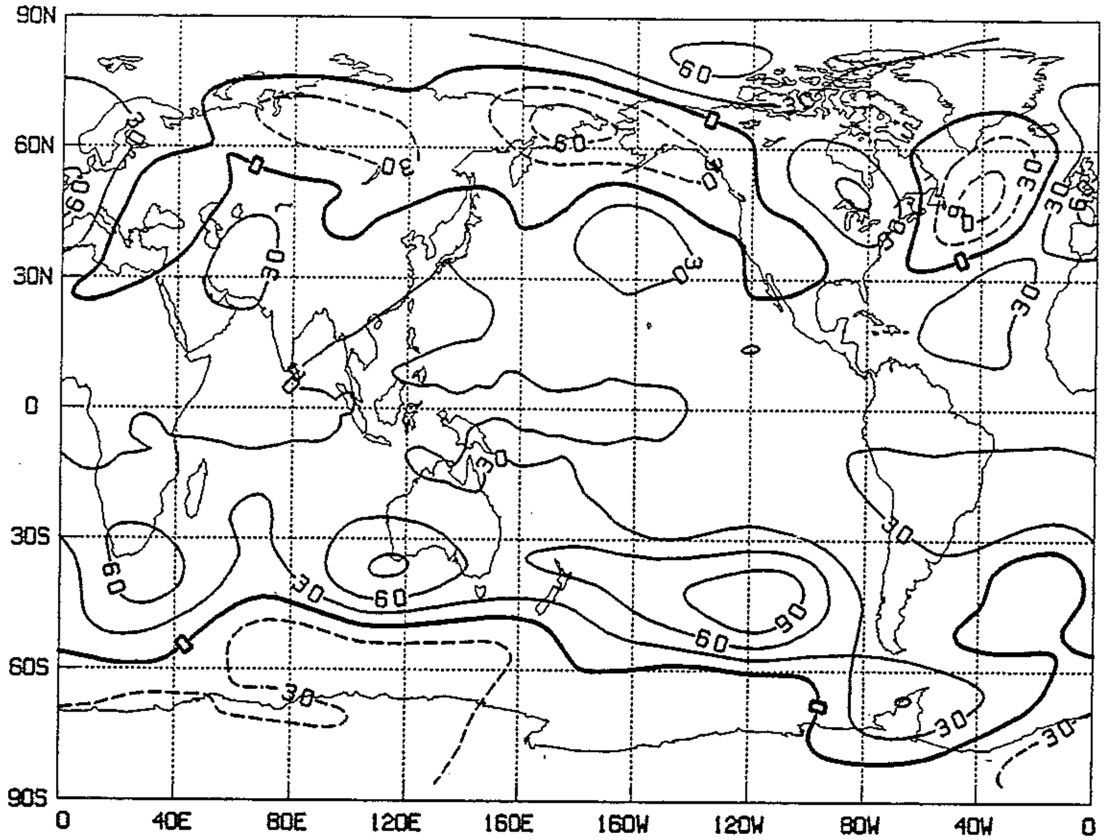

Figure 6c: MJ 1988 geopotential height at 300 mb for COLA simulated anomaly. Contour interval is 30 m. Dashed contours are negative.

GCM positive anomaly over North America is only 60 geopotential meters in magnitude and is situated 10–15° eastward of that observed. This is consistent with the eastward displaced precipitation anomalies simulated by the COLA GCM (Fig. 3c). The COLA GCM also simulates somewhat realistic 300 mb geopotential anomalies to the north and north–east of the anomalous AVD regions in the tropical Atlantic and eastern Indian – western Pacific Oceans previously noted.

The simulated anomaly fields shown were formed by subtracting the mean of the control ensemble (climatological SST) from the mean of the boundary ensemble (observed SST), and thus, include only the effect of the observed SST. To investigate whether the

GCMs otherwise simulated the geopotential height pattern associated with the 1988 US drought, we compare the departure from the zonal mean of the MJ 1988 300 mb geopotential height for the observations (Fig. 7a), the boundary ensemble mean of the

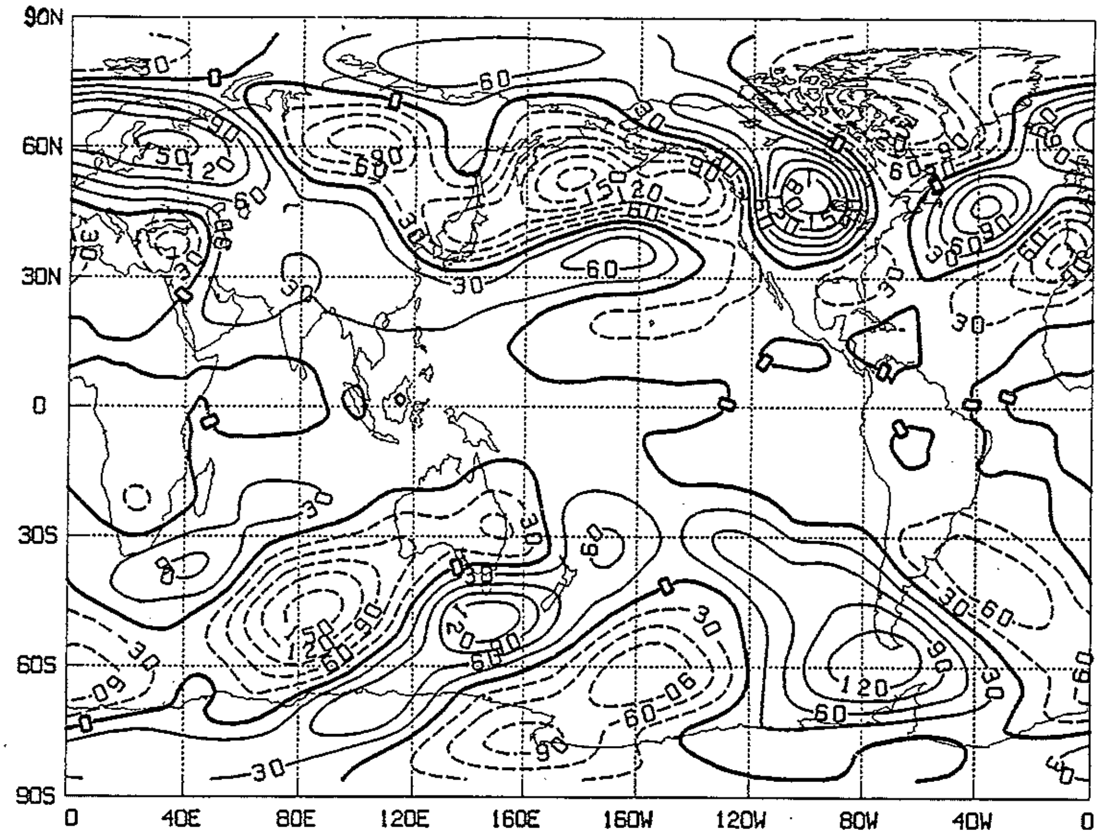

Figure 7a: MJ 1988 departure from the zonal mean of the 300 mb geopotential height for NMC observed mean. Contour interval is 30 m. Dashed contours are negative.

GLAS GCM (Fig. 7b), and the boundary ensemble mean of the COLA GCM (Fig. 7c). The GLAS GCM field bears little resemblance to that observed and has only the slightest indication of ridging over the central U.S. where a very strong (180 m) ridge was observed. The COLA GCM has a much more accurate representation of the observed waves in general, and of the ridging over the U.S. in particular, where the COLA GCM has a ridge

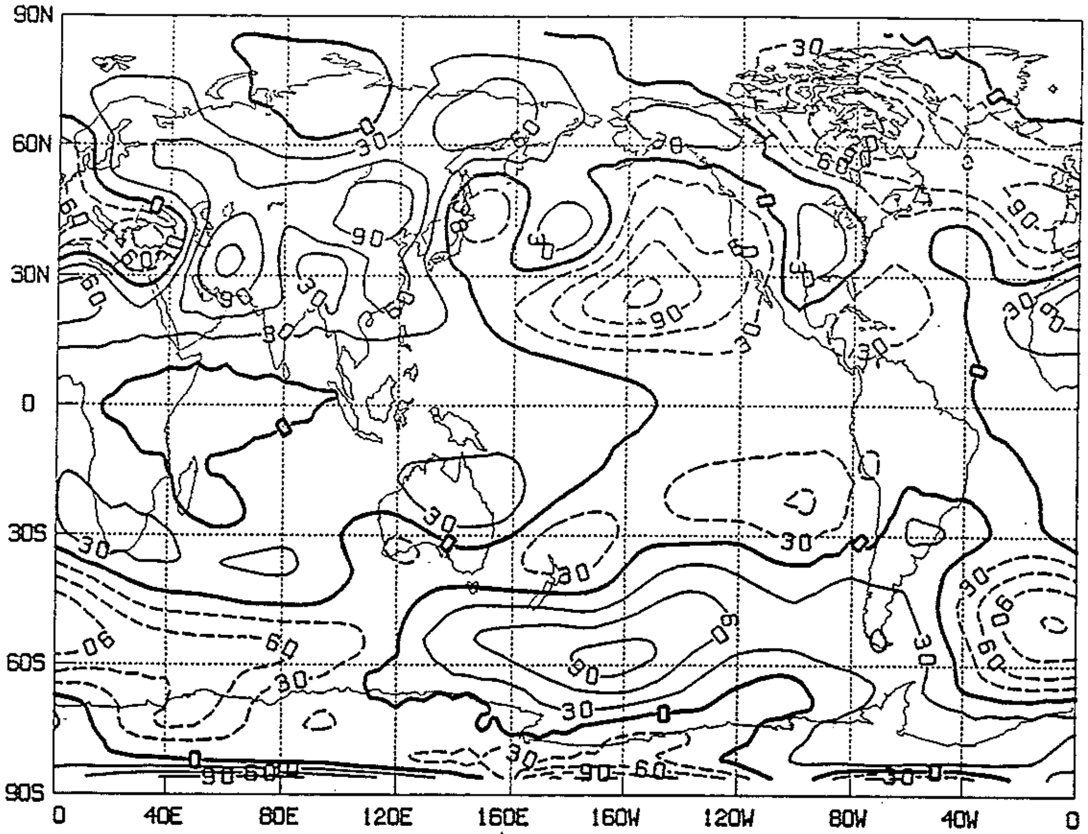

Figure 7b: MJ 1988 departure from the zonal mean of the 300 mb geopotential height for GLAS boundary ensemble mean. Contour interval is 30 m. Dashed contours are negative.

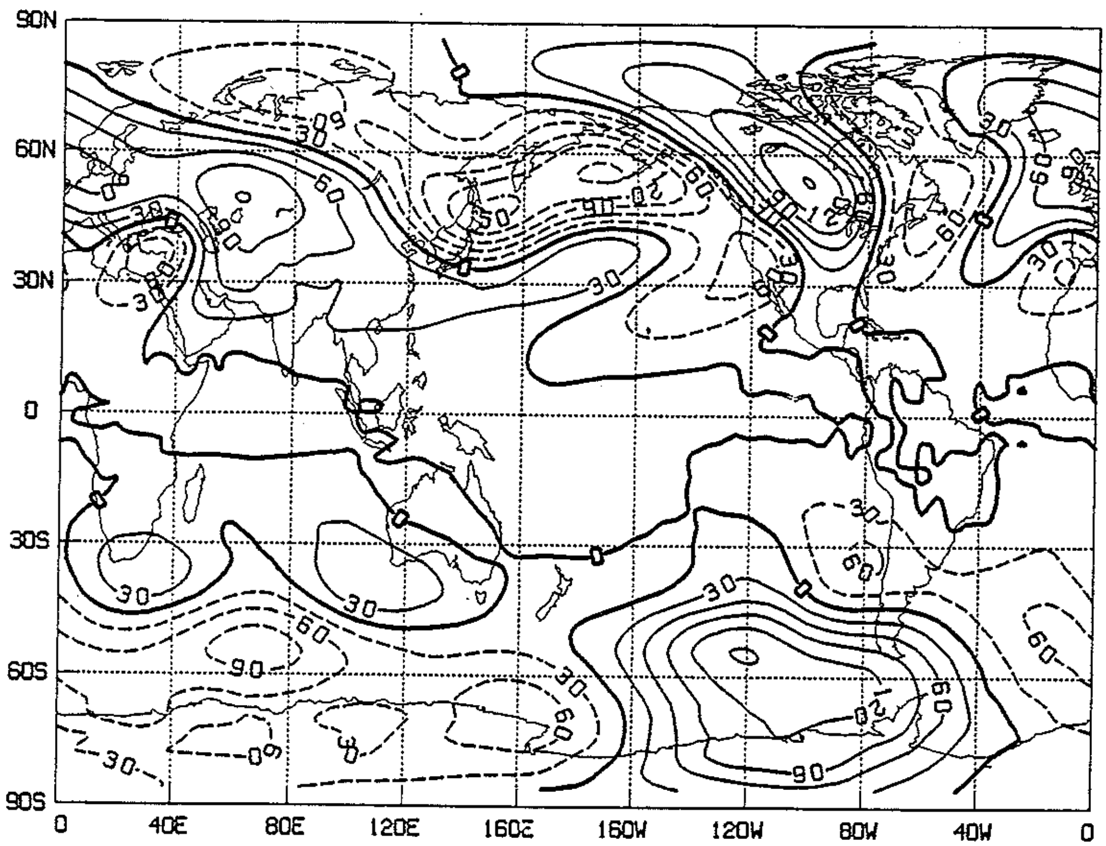

Figure 7c: MJ 1988 departure from the zonal mean of the 300 mb geopotential height for COLA boundary ensemble mean. Contour interval is 30 m. Dashed contours are negative.

reaching 150 m in magnitude. Although this ridge is still somewhat weaker than that observed, it does appear that the COLA GCM has done a fair job of simulating it.

4. SUMMARY

The experiments described here were inspired by the Trenberth et al. (1988) study which attempted to link the anomalous SST and OLR in the central and eastern tropical Pacific, to the observed upper level wave train apparently emanating from this region across North America, to the 1988 U.S. drought, all during MJ 1988. However, unlike the Trenberth et al. (1988) study, which utilized observed diagnostics and simple modeling results, these experiments were done with full atmospheric GCMs forced only by the observed SST. The SST used was global in extent, and thus the GCMs were capable of being forced by the SST anomalies observed anywhere on the globe, including those in the immediate vicinity of the OLR anomalies used by Trenberth et al. (1988).

Of the two GCMs used, we believe only the results of the COLA GCM should be taken seriously. The GLAS GCM had serious deficiencies in its time mean simulations of the MJ precipitation, upper level zonal wind, and upper level eddies. In addition, it failed to convert its tropical precipitation anomalies, which appeared reasonable, to divergence anomalies at the appropriate level in the upper troposphere. These deficiencies preclude the possibility of realistically reproducing any observed Rossby wave dispersion from the tropics and perhaps any other tropical–extra–tropical interaction as well. The COLA GCM did a good job at simulating these relevant features. The remaining discussion here will focus on the results from the COLA GCM.

The observed SST caused simulated precipitation and divergence anomalies in the central and eastern tropical Pacific similar to those observed during MJ 1988. Thus, heating anomalies similar to those used to force a simple model by Trenberth et al. (1988) have themselves been forced in the COLA GCM by inclusion of the observed SST. These heating anomalies caused simulated divergence anomalies in the upper troposphere which are associated with a Rossby wave source which apparently forced an extra–tropical wave train somewhat similar to that observed. This simulated anomalous wave train enhanced ridging over the U.S., but this anomalous ridging was eastward and weak compared to that observed. The simulated negative precipitation anomalies occurred over the Gulf Stream, rather than over the central and eastern U.S., as observed. One interpretation of these results is that the observed central and eastern tropical Pacific SST would have enhanced the simulated 1988 U.S. drought, if the COLA GCM, for reasons yet to be determined, had not shifted the responsible circulation anomaly pattern too far eastward. Even with this interpretation, the magnitude of the anomalous ridging caused by the observed SST was small compared to that observed. This result, combined with the strength of the simulated ridge at 300 mb in the ensemble mean of the boundary simulations, leads us to conclude that the observed global SST could have enhanced, but not solely caused, the 1988 U.S. drought during MJ 1988. These results do not address the role the global SST might have played in the initiation of the 1988 drought in the central and eastern U.S., which occurred during March and April.

The simulations with the COLA GCM have clearly shown that tropical SST anomalies, other than those in the central and eastern Pacific, were capable of forcing extra–tropical circulation anomalies during MJ 1988. Simulated precipitation, divergence and Rossby wave source anomalies are associated with the SST anomalies observed in the equatorial Atlantic and the equatorial western Pacific – eastern Indian Ocean regions during MJ 1988. The presence of these anomalies and their associated wave trains complicates any simple interpretation of the tropical–extra–tropical interactions during MJ 1988.

ACKNOWLEDGEMENTS

The authors would like to thank Ms. Diane Marsico of the Climate Analysis Center (CAC) for providing the SST data used in this study and Mr. Bob Kistler for providing the NMC analyses used to initialize the models and verify the model results. We would also like to thank Ms. Marlene Schlichtig for her careful preparation of the manuscript. We are indebted to NASA Goddard Space Flight Center and NMC for providing the computer time needed to complete this study. This study was supported by the NASA climate program (NAGW–557) and NSF grant ATM–8713567.

REFERENCES

Arakawa, A., 1969: Parameterization of cumulus convection. **Proc. WMO/IUGG Symp. on Numerical Prediction**, Tokyo, 1–6.

Baumhefner, D. P., J. J. Tribbia and M. L. Blackmon, 1988: The influence of specified sea surface temperature and initial condition uncertainty on Monte Carlo extended range forecast ensembles. Proc. **ECMWF Workshop on Modelling the Sensitivity and Variations of the Ocean–Atmosphere System**, WMO/TD–No. 254, WCRP–15, World Meteorological Organization, Geneva, 3–10.

Branstator, G., 1983: Horizontal Energy Propagation in a Barotropic Atmosphere with Meridional and Zonal Structure. *J. Atmos. Sci.*, **40**, 1689–1708.

Deardorff, J. W., 1972: Parameterization of the planetary boundary layer for use in general circulation models. *Mon. Wea. Rev.*, **100**, 93–106.

Fennessy, M. J. and J. Shukla, 1991: Comparison of the impact of the 1982–83 and 1986–87 Pacific SST anomalies on time mean predictions of atmospheric circulation. *J. Climate*, **3**, to appear April 1991.

Fennessy, M. J., L. Marx and J. Shukla, 1985: General circulation model sensitivity to 1982–83 equatorial pacific sea surface temperature anomalies. *Mon. Wea. Rev.*, **113**, 858–864.

Graham, N. E. and T. P. Barnett, 1987: Sea surface temperature, surface wind divergence and convection over tropical oceans. *Science*, **238**, 657–659.

Harshvardhan, and T. G. Corsetti, 1984: Longwave radiation parameterization for the UCLA/GLAS GCM. **NASA Tech. Memo. 86072**, p. 65.

Kinter III, J. L., J. Shukla, L. Marx and E. K. Schneider, 1988: A simulation of the winter and summer circulations with the NMC global spectral model. *J. Atmos. Sci.*, **45**, 2486–2522.

Kuo, H. L., 1965: On the formation and intensification of tropical cyclones through latent heat release by cumulus convection. *J. Atmos. Sci.*, **22**, 40–63.

Lacis, A. A. and J. E. Hansen, 1974: A parameterization for the absorption of solar radiation in the earth's atmosphere. *J. Atmos. Sci.*, **31**, 118–133.

Randall, D. A., 1976: The interaction of the planetary boundary layer with large–scale circulations. Ph.D. thesis, University of California, Los Angeles, pp. 247.

Sardeshmukh, P. D. and B. J. Hoskins, 1988: On the generation of global rotational flow by steady idealized tropical divergence. *J. Atmos. Sci.*, **45**, 1228–1251.

Sela, J. G., 1980: Spectral modeling at the National Meteorological Center. *Mon. Wea. Rev.*, **108**, 1279–1292.

Shukla, J. and M. J. Fennessy, 1988: Prediction of time–mean atmospheric circulation and rainfall: Influence of Pacific sea surface temperature anomaly. *J. Atmos. Sci.*, **45**, 9–28.

Tiedtke, M., 1984: The effect of penetrative cumulus convection on the large–scale flow in a general circulation model. *Beitr. Phys. Atmos.*, **57**, 216–239.

Trenberth, K. E., G. W. Branstator and P. A. Arkin, 1988: Origins of the 1988 North American Drought. *Science*, **242**, 1640–1645.

Webster, P. J. and J. R. Holton, 1982: Cross equatorial response to middle latitude forcing in a zonally varying basic state. *J. Atmos. Sci.*, **39**, 722–733.